Rotational dynamics of proteins from spin relaxation times and molecular dynamics simulations

O. H. Samuli Ollila*
Insititute of Biotechnology, University of Helsinki and
Institute of Organic Chemistry and Biochemistry, Czech Academy of Sciences, Prague 6, Czech Republic

Hideo Iwai
Insititute of Biotechnology, University of Helsinki
(Dated: June 21, 2017)

I. INTRODUCTION

Protein conformational sampling and entropy play a significant role in protein functionality and interactions with other biomolecules. In addition to internal dynamics due to conformation sampling, the proteins also experience overall brownian tumbling. These properties are experimentally accessible through spin relaxation times of ^{15}N and ^{13}C nucleai measured with nuclaer magnetic resonance (NMR) techniques [1–5]. Spin relaxation rate experiments have been used to, for example, analyze conformational entropies [1, 6, 7], binding entropies [1, 8], resolve sampled structures [3] and validate molecular dynamics simulations [9–13]. These analyzes are almost exclusively based on the separation of internal conformational sampling and overall rotational tumbling [14, 15] and often isotropic diffusion for overall tumbling is assumed, while analysis of anisotropic molecules significantly more complicated [1, 2, 16, 17]. Thus, new methods are needed to intepret spin relaxation times measured from samples with anisotropic or intrinsically disordered molecules.

Classical molecular dynamics simulation methods are promising tools to interpretate spin relaxation time experiments for molecules with significant anisotropy or correlations between internal and overall rotational motions. However, practical applications are often limited by inaccuracies in the force field descriptions and available time scales in the simulations [12, 13, 18, 19]. The most used water model in rotational dynamics studies, tip3p [20], predicts too fast rotational diffusion [21]. On the other hand, very long simulations are needed to collect enough statistics to calculate rotational correlation functions from single molecules in MD simulations [19, 22]. Consequently, overall rotational diffusion of protein rotational diffusion is not typically analyzed from atomistic resolution simulation data. Instead, the calculated relaxation rates are fitted to experiments by assuming an isotropic diffusion model [**?**].

In this work we overcome these issues by directly calculating diffusion coefficients from protein intertia axes. Diffusion coefficients can be then used to determine global rotational correlation functions from shorter simulations than with direct calculation. Furthermore, the oversestimated dynamics due to water model can be anisotropically corrected by scaling the diffusion coefficients with a constant factor. The usefullness of the approach is demonstrated by interpreting the spi

relaxation data from aniotropic protein constructs from TonB of Helicobacteri pyroli [**?**] and Pseudomonas [**?**]. These segments are considered as vital parts related to iron transport into Gran-negative bacteria [**?**].

II. METHODS

A. Spin relaxation and rotational dynamics of molecules

Two different approaches have been commonly used to analyze rotational dynamics from NMR relaxation experiments. In "model free analysis" the fundamental idea is to separate interal dynamics from global rotation and assume exponential forms for rotational correlation functions. The parameters of rotational correlation functions are then fitted the experimental data to solve time scales and order parameters for different dynamical processes [23**?**]. Alternative approach is to use bead models and hydrodynamical calculations to describe protein dynamics and predict spin relaxation rates [24]. The approaches have been successfull or several proteins, but both suffer from significant limitations which limit the general applicability [**?**]. Main practical issue in the "model free analysis" is that the amount of freen parameters to be fitted in the experiments becomes large for anitropic proteins experiencing complex dynamics [**?**]. On the other hand, hydrodynamical calculations are sentitive for the assumptions about protein hydration shell [24].

Spin relaxation data is usually analyzed by describing the sampled bond orientations with order parameter S^2 respect to the protein reference frame and assuming that overall and internal motions are independt [2**?**]. Order parameters and timescales for overall and internal motions can be then extracted by fitting various functional forms to spin relaxation data measured with different magnetic field strengths [1, 2].

Practical approaches to analyze molecular dynamics from NMR relaxation data are usually based on the connection between second order rotational correlation function $C(t)$ of N-H bond and experimentally measured spin relaxation rates R_1, R_2 and R_{NOE} through Redfield equations [25, 26]

$$R_1 = \frac{d_{\mathrm{NH}}^2 N_{\mathrm{H}}}{20}\left[J(\omega_{\mathrm{H}} - \omega_{\mathrm{N}}) + 3J(\omega_{\mathrm{N}}) + 6J(\omega_{\mathrm{N}} + \omega_{\mathrm{H}})\right]$$
$$+ \frac{(\sigma\omega_{\mathrm{N}})^2}{15}j(\omega_{\mathrm{N}}),$$

$$(1)$$

* samuli.ollila@helsinki.fi

$$R_2 = \frac{1}{2} \frac{d_{\text{NH}}^2 N_{\text{H}}}{20} \Big[4J(0) + 3j(\omega_{\text{N}}) + J(\omega_{\text{H}} - \omega_{\text{N}}) + 6J(\omega_{\text{H}})$$
$$+ 6J(\omega_{\text{N}} + \omega_{\text{H}}) \Big] + \frac{(\sigma \omega_{\text{N}})^2}{15*6} [4J(0) + 3J(\omega_{\text{N}})], \tag{2}$$

$$R_{\text{NOE}} = 1 + \frac{d_{\text{NH}}^2 N_{\text{H}}}{20} \Big[6J(\omega_{\text{N}} + \omega_{\text{H}}) + J(\omega_{\text{H}} - \omega_{\text{N}})) \Big] \frac{\gamma_{\text{H}}}{\gamma_{\text{N}} R_1}, \tag{3}$$

where ω_{N} and ω_{H} are the Larmor angular frequencies of ^{15}N and ^{1}H respectively, and N_{H} is the number of bound protons. Spectral density $J(\omega)$ is the Fourier transformation of the second order rotational correlation function for N-H bond

$$J(\omega) = 2 \int_0^\infty C(t) \cos(\omega t) \mathrm{d}t. \tag{4}$$

The second order rotational correlation is defined as

$$C(t) = \langle (3\cos^2 \theta_{t';t'+t} - 1)/2 \rangle_{t'}, \tag{5}$$

where average is ensemble average and θ is the angle between N-H bonds at times t' and $t'+t$. The dipolar coupling constant is given by

$$d_{\text{NH}} = -\frac{\mu_0 \hbar \gamma_{\text{H}} \gamma_{\text{N}}}{4\pi \langle r_{\text{CN}}^3 \rangle},$$

where μ_0 is the magnetic constant or vacuum permeability, $\hbar$ is the reduced Planck constant, γ_{N} and γ_{H} are the gyromagnetic constants of ^{15}N and ^{1}H, respectively. Average cubic length is $\langle r_{\text{CN}}^3 \rangle \approx$ and the chemical shift anisotropy is $\Delta\sigma \approx 160 * 10^{-6}$ for N-H bonds in proteins [?]. Same equations can be used, for example, to C-H bond by changing the constants related to nitrogen to the ones corresponding carbon.

Experimental spin relaxation rates of proteins are typically intepreted by assuming that the global and interal rotational dynamics are independent. The rotational correlation function for each bond can be then written as [?]

$$C(t) = C_I(t)C_O(t), \tag{6}$$

where $C_I(t)$ and $C_O(t)$ are correlation functions for internal and overall rotiations, respectively. Within this approximation the internal rotational correlation function decays to a plateau, which defines the square of order parameter respect to molecular axes S^2. Timescale for internal relaxation dynamics can be estimated by using the effective internal correlation time

$$\tau_{\text{eff}} = \int_0^\infty C_I'(t) \mathrm{d}t, \tag{7}$$

where $C_I'(t) = (C_I - S^2)/(1 - S^2)$ is the reduced correlation function [?].

The global rotational dynamics for fully anisotropic molecule can be described as a sum of five exponentials

[2, 27]

$$C_O(t) = \sum_{j=1}^5 A_j e^{-t/\tau_j}, \tag{8}$$

where time constants τ_j are related [28] to the diffusion constants around three principal axes of a molecule (D_{xx}, D_{yy} and D_{zz}) and prefactors A_j can be related to the directions of bond respect to the principal axes. The rotational diffusion constants are defined as

$$\langle (\Delta\alpha_{t';t'+t})^2 \rangle_{t'} = 2D_{xx}t$$
$$\langle (\Delta\beta_{t';t'+t})^2 \rangle_{t'} = 2D_{yy}t \tag{9}$$
$$\langle (\Delta\gamma_{t';t'+t})^2 \rangle_{t'} = 2D_{zz}t,$$

where $\langle (\Delta\alpha_{t';t'+t})^2 \rangle_{t'}$, $\langle (\Delta\beta_{t';t'+t})^2 \rangle_{t'}$ and $\langle (\Delta\gamma_{t';t'+t})^2 \rangle_{t'}$ are mean square angle deviations of protein intertia axes.

The internal and overall correlation functions are monoexponential for proteins with isotropic overall rotational diffusion and single timescale for internal motion. The dynamics of such proteins is described with three parameters in the original "model free analysis"; internal rotational relaxation time τ_e, global rotaional relaxation time τ_c and the order parameter S^2. The values for these parameters can be then determined by fitting the Eqs. 1-8 to experimental spin relaxation data [?]. However, the amount of exponentials needed to describe correlation functions, and thus the free parameters, in such fit increases if proteins experience anisotropic overall diffusion or several internal timescales. Thus the "model free analysis" becomes less applicable for proteins with significant anisotropy or more complicated internal dynamics.

B. Rotational dynamics from molecular dynamics simulations

Classical molecular dynamics simulation gives a trajectory for each atom in a system as a function of time. These trajectories can be used to calculate rotational correlation functions for each bond from Eq. 5. The rotational correlation functions can be further used to calculate the spin relaxation times through Eqs. 1-4 and the resulting values can be compared to experimental data in order to assess simulation model quality [?] and interpret experiments [?]. However, the comparison is often complicated by the short simulation times [?] and incorrect overall rotational diffusion due to water models [?].

Here we use overall rotational diffusion constants calculated from Eq. 9 to determine the timescales of global rotational correlation function in Eq. 8. The rotational diffusion coefficients are given by a linear fit to the mean square angle deviation of intertia axes calculated from simulations (see results and discussion). Straight line has only one parameter (slope) to be fitted, in contrast to multiexponential sum in Eq. 8 with ten parameters. Thus, the calculation of timescales through overall rotational diffusion constants is numerically more robust and requires less simulation data than a direct fit of Eq. 8 to the rotational correlation function calculated from simulation. The prefactors in 8 are determined by fit-

ting to correlation function calculated from simulations, but timescales from rotational diffusion coefficients are used. The rotational diffusion constants can be also scaled with a constant factor and new correlation functions calculated to compensate the incorrect rotational diffusion due to water model in spin relaxation rate calculations.

The analysis can be divided in essentially six steps:

1) Total rotational correlation functions $C(t)$ for protein N-H bonds are calculated from MD simulation trajectory by applying Eq. 5.

2) Rotational correlation functions for internal dynamics $C_I(t)$ are calculated from a trajectory from where the overall rotation of protein is removed.

3) The overall and internal motions are assumed to be independent and overall rotational correlation function is calculated as $C_O(t) = C(t)/C_I(t)$ according to Eq. 6.

4) The protein axes of inertia and their mean square deviations as function of time are calculated from MD simulation trajectory.

5) Rotational diffusion constants D_x, D_y and D_z are calculated by fitting a straight line to mean square angle deviations of inertia axes according to Eq. 9.

6) Timescales in Eq. 8 are calculated from diffusion constants and weighting factors A_j are determined by fitting the equation to rotational correlation functions of overall rotational motion $C_0(t)$ determined in step 3.

7) New total rotational correlation functions based on Eqs. 6 and 8 are determined as

$$C_N(t) = C_I(t) \sum_{j=1}^{5} A_j e^{-t/\tau_j}, \qquad (10)$$

where internal correlation function $C_I(t)$ is taken from step 2, τ_i values from rotational diffusion constants (step 5) and prefactors A_j from step 6. The incorrect rotational diffusion due to water model can be compensated in new correlation functions at this point by scaling the rotational diffusion coefficients with a constant factor.

C. Simulation and analysis details

Simulations were ran using Gromacs 5 [29] And Amber ff99SB- ILDN [30] force field for proteins . The proteins were solvated to tip3p[20], tip4p [20] or OPC4 [31] water models. NMR structures from [?] and [32] are used as initial structure for PaTonB and HpTonB-92, respectively. Temperature was coupled to desired value with v-rescale thermistat [33] and pressure was isotropically set to 1 bar using Parrinello-Rahman barostat [34]. Timestep was 2 fs, Lennart-Jones interactions were cut-off at 1.0 nm, PME [35, 36] was used for electrostatics and LINCS was used to constraint all bond lengths [37]. Simulation trajectory and related files are available at [??]. The simulated systems are listed in Table I

Rotational correlation functions are calculated with *gmx rotacf* and overall rotation for $C_I(t)$ calculation is removed by using fit option in *gmx trjconv* grom Gromacs package [38]. Inertia axes of protein for rotational diffusion calculation are

calculated with *compute_inertia_tensor* from MDTraj python library [39]. For spectral density calculation a sum of 471 exponentials having correlation times from 1 ps to 50 ns with logarithmic spacing

$$C_N(t) = \sum_{i=1}^{N} \alpha_i e^{-t/\tau_i} \qquad (11)$$

were fitted to the new correlation function calculated from Eq. 10 by using the *lsqnonneg* routine in MATLAB [40]. The Fourier transform is then calculated by using analytical function for the sum of exponentials

$$J(\omega) = 4 \sum_{i=1}^{N} \alpha_i \frac{\tau_i}{1 + \omega^2 \tau_i^2}. \qquad (12)$$

Similar approach is used previously for lamellar systems in combination with solid state NMR experiemnts [41, 42].

III. RESULTS

A. Global rotational dynamics of protein

The mean square angle deviations for protein inertia axes as a function of time are shown in Fig. 1 for PsTonB simulation with OPC4 water model, which the longest data set in this work (1.2μs). Linear behaviour of root mean square angle deviations are observed for the lag times up to 12 ns, suggesting that the protein follows linear diffusion model with a good approximation. Plot with log-log scale in Fig. **??** B) reveals a weakly subdiffusive region only below very short timescales of approximately 0.12 ns. Deviations from linear behaviour are also seen with longer lag times than the one hundreth of the simulation lenght as demonstrated for shorter simulations in Figs. 9 ans 8. This is expected to be the maximum lag time for a good statistics for rotational dynamics analyzed from a single molecule in MD simulations [22]. Thus, we conclude that the rotational diffusion coefficients of protein can be calculated from the slope of mean square angle deviations according to Eq. 9 by using lag times less than one hundreth of the total MD simulation length.

The resulting rotational diffusion constants from different simulations are shown in Table I. The values are in line with previously reported experimental and simulation results for different proteins with similar size [21, 43]. As expected, rotational diffusion coefficients increase with the temperature and decrease with the size of a protein. Exceptionally large diffusion constants from simulations with tip3p water model are also previously observed and explained with overestimated water self diffusion [21].

The calculated rotational diffusion constants can be used to determine the timescales in Eq. 8 for the overall rotational dynamics of a protein, while prefactors in the equation depend on the orientations of the each N-H bond respect to intertia axes in a complicated way [16, 27]. Here we determine the prefactors by fitting Eq. 8 with the timescales given

TABLE I. Simulated systems and rotational diffusion coefficients (rad$^2 \cdot 10^7$/s) calculated from simulations.

| Protein	Water model	T (K)	t_{sim} (ns)	t_{anal} (ns)	D_{xx}	D_{yy}	D_{zz}	$D_{||}/D_+$	D_{av}	files
PaTonB	tip4p	298	400	390	1.81 ± 0.01	2.06 ± 0.03	4.55 ± 0.03	2.35 ± 0.04	2.80 ± 0.02	[?]
PaTonB	tip4p	310	400	390	2.60 ± 0.02	2.22 ± 0.05	5.0 ± 0.1	2.07 ± 0.09	3.26 ± 0.07	[?]
PaTonB	OPC4	310	1200	1190	2.01 ± 0.01	2.19 ± 0.01	5.01 ± 0.03	2.39 ± 0.02	3.07 ± 0.01	[?]
HpTonB-92	tip3p	310	570	370	8.25 ± 0.05	7.67 ± 0.06	15.9 ± 0.3	1.99 ± 0.06	10.6 ± 0.2	[?]
HpTonB-92	tip3p	303	800	790	6.24 ± 0.02	7.04 ± 0.03	11.9 ± 0.2	1.80 ± 0.03	8.40 ± 0.07	[?]
HpTonB-92	tip4p	310	470	370	3.6 ± 0.1	3.24 ± 0.01	6.3 ± 0.3	1.8 ± 0.1	4.4 ± 0.2	[?]
HpTonB-92	tip4p	303	400	200	2.7 ± 0.1	2.71 ± 0.02	5.6 ± 0.5	2.1 ± 0.2	3.7 ± 0.2	[?]
HpTonB-92	OPC4	310	800	790	2.85 ± 0.01	2.70 ± 0.01	5.56 ± 0.01	2.00 ± 0.01	3.70 ± 0.01	[?]
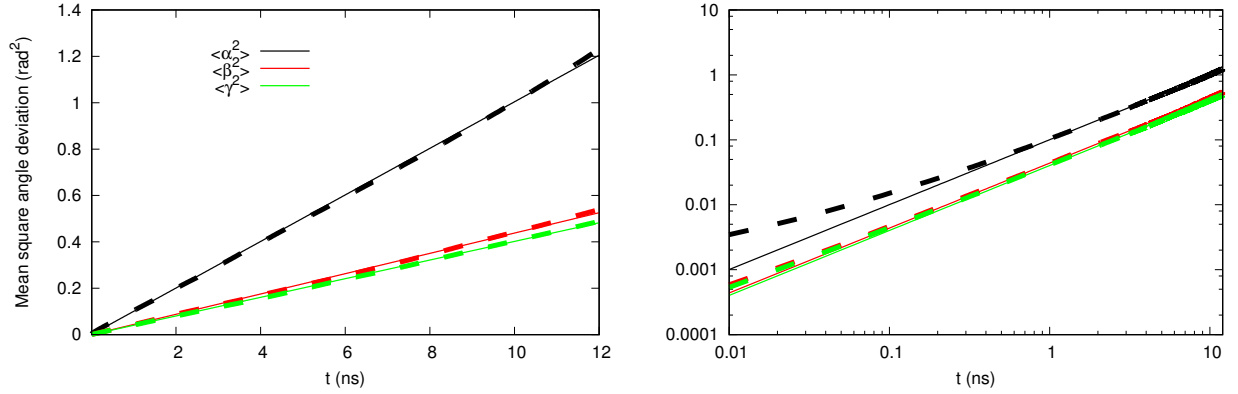
FIG. 1. The intertia tensor angles as a function of time and mean square angular deviations for PsTonB simulation with OPC water model.

by diffusion coeffiecients to the overall rotational correlation function calculated from MD simulations. The prefactors and timescales for overall rotational correlation functions can be then combined with internal correlation function calculated from oriented MD simulations to determine the new correlation functions from Eq. 10. The new correlation function has less fluctuations with longer time scales, thus giving more robust spin relaxation times.

The rotational correlation function analysis is exemplified in Fig. 2 for residues in different parts of PsTonB having different features in rotational dynamics. Flexible C-terminus is represented by residue 341, more rigid β-sheet by residue 331 and a flexible loop between two sheets by residue 322. The total correlation functions $C(t)$ calculated from original MD trajectories, shown in Fig. 2 A) (solid lines), decay toward zero within ~10-50 ns. Internal correlation functions $C_I(t)$ calculated from trajectory with overall protein rotation removed, shown in Fig. 2 B), decay to a plateau value, which defines the square of the order parameter S^2. As expected, the β-sheet residue 331 has the largest order parameter value and fastest decay to it, while order parameters for loop and C-terminus are significantly smaller and deacay is slower due to larger conformational ensemble sampled by these regions. The overall rotational correlation functions $C_O(t)$ for a protein, determined as $C_O(t) = C(t)/C_I(t)$, are shown in Fig. 2 C) (solid lines).

The overall rotational correlation functions from Eq. 8 are also shown in Fig. 2 C) (dashed lines). The timescales τ_i were determined from rotational diffusion constants [28] in Table I and prefactors A_j were determined by fitting to the MD simulation data. The determined parameters were combined with internal correlation function from MD simulations by using Eq. 10 to determine new total correlation functions, which are also shown in Fig. 2 A) (dashed lines). The fitted correlation functions are indistinguishable from MD simulation results with lag times shorter than one hundredth of total simulation time (approximately 4-12ns for the studied systems), which is the expected limit for a good statistics in single molecule MD simulations [22]. Exceptionally large statistical fluctuations for overall rotational correlation function of flexible C-terminus (residue 341) with longer lag times are observed, because small contribution of overall rotation dynamics is difficult to detect with high accuracy for segments with small order parameters.

Good agreement between correlation functions from Eq. 10 with overall rotational timescales from diffusion coefficients and MD simulations, suggest that the anisotropic diffusion model (Eq. 8) and separation of internal and global motions (Eq. 6) are good approximations for the studied system. Thus, we conclude that the determined new correlation functions can be then used to reduce the influence of statistical fluctioations arising from long time scale dynamics on spin relaxation
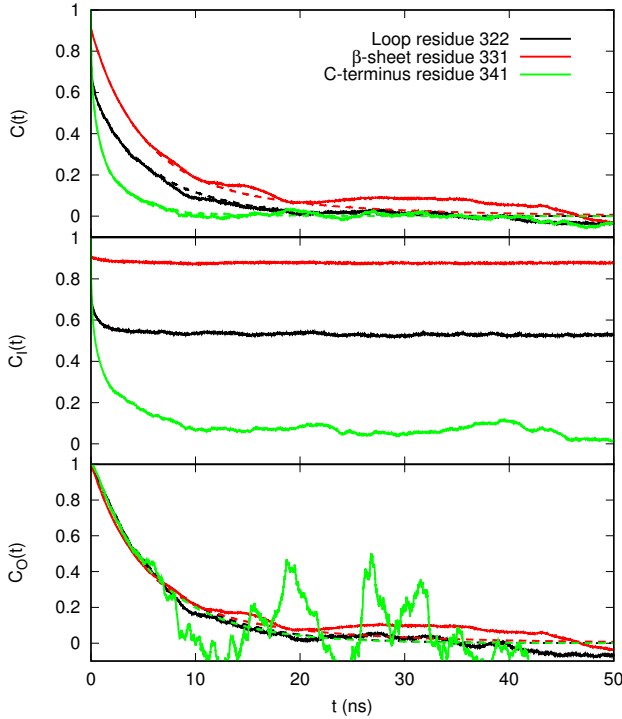
FIG. 2. Rotational correlation functions calculated from MD simulations of PsTonB with tip4p water model at 298K for residues at different regions. A) total correlation functions $C(t)$ calculated from MD simulation (solid lines) and new correlation functions determined from Eqs. 6 and 8 by using rotational diffusion constants and fitted prefactors (dashed lines), B) correlation functions for internal motions calculated from simulation with removed overall protein rotation C) correlation function for overall motions determined as $C_O(t) = C(t)/C_I(t)$ (solid lines) and by fitting to Eq. 8 with timescales from rotational diffusion coefficients in Table I (dashed lines).

time calculations from MD simulations. In addition, incorrect overall diffusion can be corrected post-simulationally in this calculation by scaling the diffusion coefficins when calculating new correlation functions. This analysis is exemplified for PsTonB and HpTonB-92 proteins in sections below.

B. Global rotational dynamics in simulations and experiments

Rotational correlation functions from simulations were determined by using Eq. 10, where internal correlation functions were taken from MD simulations, timescales were determined from protein overall rotation diffusion constants and prefactors from the fit to the MD simulation data, as decribed in previous section. The correlation functions were used to calculate spectral densities from Eqs. 11-12 and spin relaxation times were then calculated from Eqs. 1-3.

Spin relaxation time results for HpTonB-92 in Fig. 3 show a good agreement between simulation with tip4p water model and experiments. However, the results from simulation with tip3p water model are significantly off from experiments. The

underestimated T_1/T_2 ratio suggests too fast overall rotational diffusion dynamics [44] with tip3p water, in agreement with previous studies [21]. Indeed, division of diffusion constants by a constant factor of 2.9 before applying Eq. 10 brings spin relaxation times in good agreement with experiments, as shown in Fig. 4.
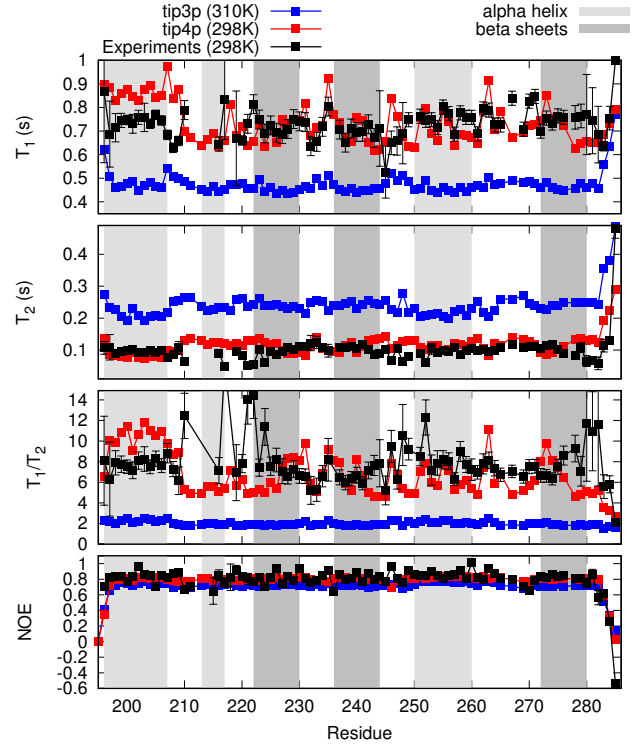

FIG. 3. Spin relaxation times for HpTonB-92 from experiments [?] and simulations with different water models.

Simulations of PsTonB with tip4p or OPC4 water models, shown in Fig. 5, give systemically smaller T_1 values and T_1/T_2 ratio than experiments. The effect of temperature difference of 12 degrees is significantly smaller than the different with experiments. Dividing the diffusion coefficients with a constant factor of 1.2 gives a good agreement for spin relaxation rates between tip4p simulation and experiments at 298K, as seen in Fig. 6.

The good agreement between spin relaxation data from experiments and simulations with scaled diffusion coefficients suggests that the values can be used to interpret the anisotropic diffusion of these proteins from the measured NMR data. The scaled rotational diffusion coefficients from MD models giving the best agreement with experimental spin relaxation data are shown in Table I. The scaled diffusion coefficients from tip3p simulations were chosen for HpTonB-92, because they give slightly better overall agreement with experiments than simulations with tip4p water model. The results are in line with values for more isotropic proteins, which are previously determined by different methods to interpret the spin relaxation data [43].
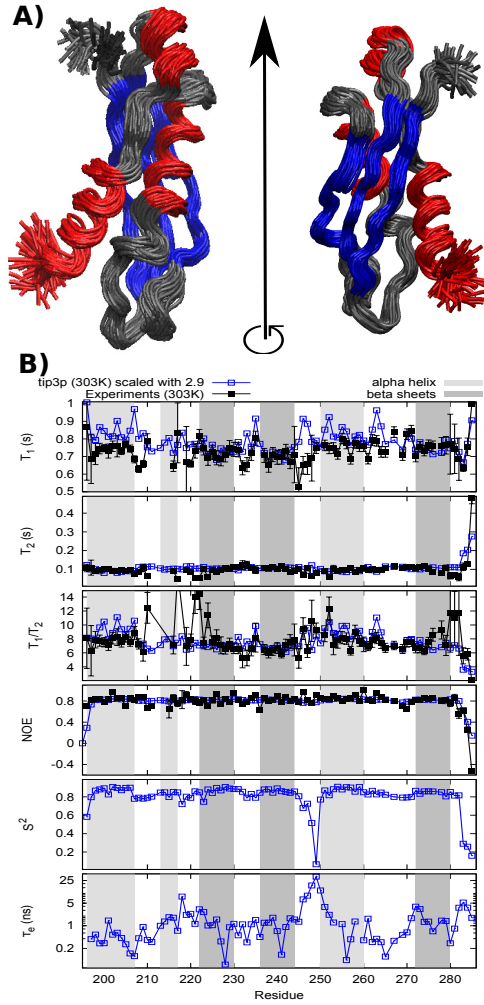
FIG. 5. Spin relaxation times for PsTonB from experiments [**?**] and simulations with different water models.

TABLE II. Rotational diffusion coefficients scaled with constant factor which gives a good agreement for spin relaxation data, 2.9 for tip3p simulation of HpTonB and by 1.2 for tip4p simulation of PsTonB.

	HpTonB-92	PsTonB
D_{xx}	2.15 ± 0.01	1.51 ± 0.01
D_{yy}	2.43 ± 0.01	1.72 ± 0.03
D_{zz}	4.10 ± 0.01	3.79 ± 0.03
D_{av}	2.90 ± 0.03	2.3 ± 0.02
τ_c(ns)	5.7 ± 0.1	7.2 ± 0.1

FIG. 4. A) Structures sampled by HpTonB-92 from MD simulations with tip3p at 303 K (100 structures from 400ns long trajectory). Secondary structures are colour labelled with Visual Molecular dynamics [45, 46]; α-helices are red and β-sheets are blue. B) Spin relaxation times from experiments and tip3p simulations with rotational diffusion coefficients divided by a constant factor of 2.9 at 303 K. Order parameters and effective internal correlation times calculated from simulations

C. Interpretation of protein internal relaxation from MD simulations

Experimental spin relaxation times are well reproduced by MD simulation data when overall rotational diffusion is scaled with a constant factor, as seen in Figs. 4 and 6. Thus, the simulations can be used to interpret internal relaxation processes observed in spin relaxation experiments for proteins.

NMR experiments and the most realistic MD simulation based model show very little variation between spin relaxation times for different residues in HpTonB-92 as seen in
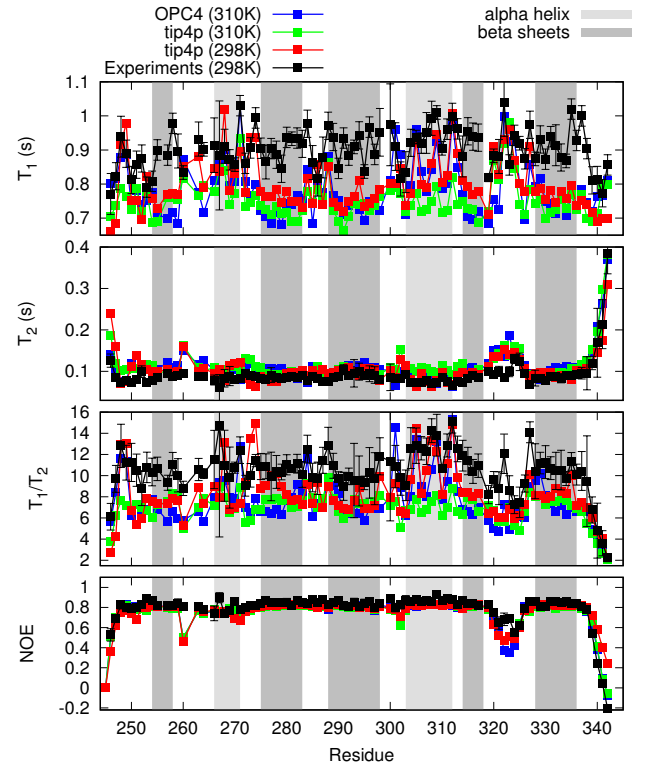
Fig. 3. This indicates a rigid protein structure, which is also seen in MD simulation snapshots overlaid in Fig. 3 A). Enhanced conformational sampling is seen only for few residues in terminal ends, which are also visible in spin relaxation data. Some deviation from average spin relaxation times are observed also between residues 210-222, which probably arises from sampling between two orientations of the α-helix (see discussion below and in Ref. [**?**]). Exceptionally low order parameters and long effective correlation times are also observed for residues 245-250 in simulations and the same region gives small T_1 times in experiments. However, the interpretation of these observations is not straightforward, because low T_1 in this region are not reproduced by simulations. More detailed discussion together with longer HpTonB construct is presented elsewhere [**?**].
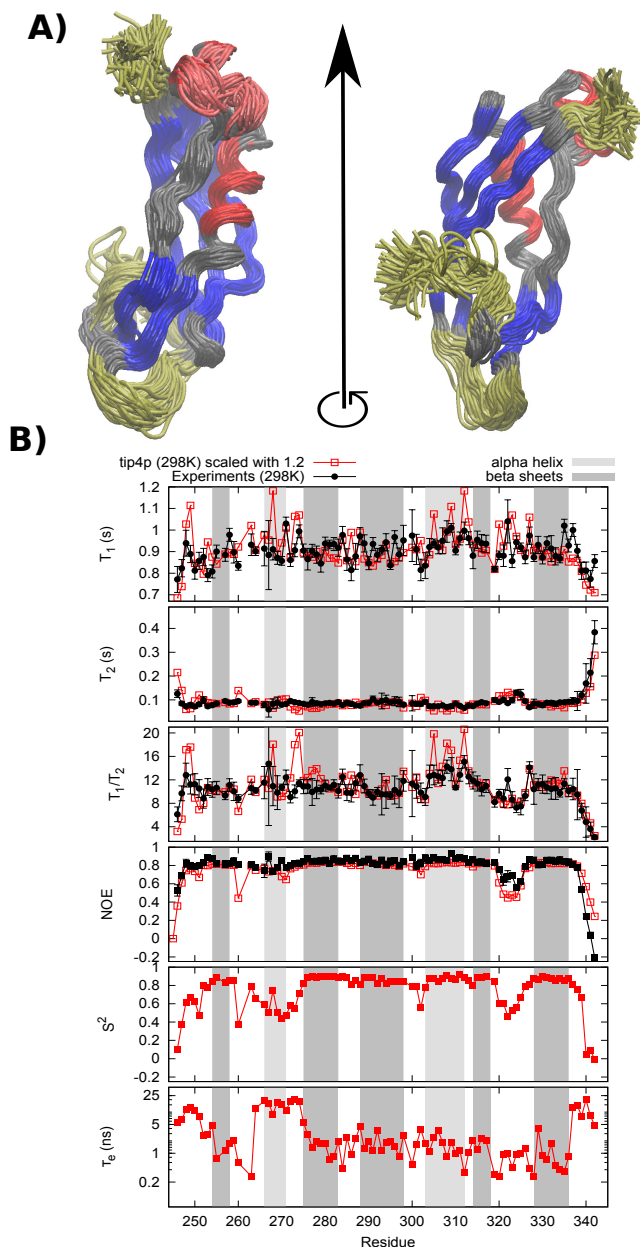
More variety in internal dynamics between residues is

simulations and experiments. The terminal ends are also characterized by low order parameters and long effective internal correlation times arising from larger amount of sampled conformational states. Enhanced conformational sampling is also observed for residues between 320-326, which is a loop between two β-sheets. Low order parameters and long internal effective correlation times are also observed in MD simulations for residues between 260-274, which similar region as residues 210-222 in HpTonB-92. In this case the simulations reveal two different orientations sampled by the α-helix in this region (colour labelled with pink in Fig. 5 A)), which also explains the lower resolution in NMR spectra for this region observed for PsTonB and HpTonB constructs [**?**].

Relaxation processes can be further quantified by analysing the timescales, which lead to spin relaxation times in agreement with experiments. This is exemplified in Fig. 7 by plotting the prefactors corresponding each timescale after fitting Eq. 11 to MD simulation data. The same residues for PsTonB as in Fig. 2 are used. Rotational relaxation of residue 331 in β-sheet is dominated by timescales of $\sim$5.5 ns and $\sim$8 ns, which arise from global rotation of protein. Only a small fraction of relaxation arises from fast internal motions, as expected for rigid structure with large order parameter value. Rotational relaxation of residue 322 in flexible loop is also dominated by timescales around $\sim$8 ns corresponding overall rotational diffusion, but fast motions related to internal protein dynamics are more significant than for the β-sheet residue in agreement with lower order parameter value. On the other hand, rotational dynamics of residue 341 in N-terminal is dominated by timescales below 3 ns related to the internal protein relaxation. The contribution from timescales close to $\sim$13 ns is probably related to slow conformational sampling of N-terminus, rather than overall rotational dynamics. This is in agreement with Fig. 5, suggesting that sampling of large amount of conformations leads to small order parameters and large effective correlation times.
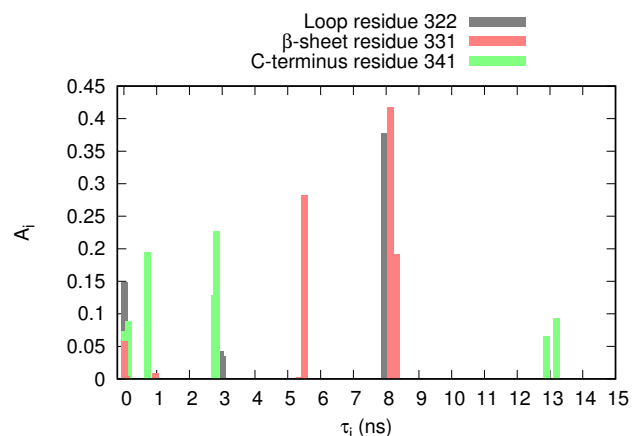

FIG. 6. A) Structures sampled by PsTonB from MD simulations with tip4p at 298 K (100 structures from 400ns long trajectory). Secondary structures are colour labelled with Visual Molecular dynamics [45, 46]; α-helixces are red and β-sheets are blue. Residues 246-251, 320-326 and 338-342 with increased internal dynamics are yellow and α-helix sampling between two orientations (residues 266-270) is pink in the left column. B) Spin relaxation times from experiments and tip4p simulations with rotational diffusion coefficients divided by a constant factor of 1.2 at 298 K. Order parameters and effective internal correlation times calculated from simulations.

found for PsTonB protein, as seen in Fig. 6. Segments with enhanced conformational sampling are labelled with yellow colour in Fig. 6 A). The terminal ends show significantly enhanced conformational sampling in MD simulation snapshots, which is also observed in spin relaxation times from

FIG. 7. Prefactors A_i corresponding different timescales τ_i in Eq.11 from correlation functions giving a good agreement with experimental spin relaxation times for PsTonB at 298K.

IV. DISCUSSION AND CONCLUSIONS

Protein rotational dynamics was separated to the overall brownian tumbling around protein intertia axes and internal conformational sampling. The overall rotational diffusion constants were calculated from the slope of mean square angle deviations (Eq. 9), which were found to be essentially linear for all inertia axes. The results indicate that monomeric proteins in dilute solution experience rotational brownian tumbling in agreement with previous MD simulation study [21]. Only a small subdiffusive behaviour was found with short timescales below 0.12 ns. This result can be used as a constrast for crowded environment, where anomalous diffusion is expected to be more significant [47].

General form of rotational correlation function for anisotropic rigid body (Eq. 8) with timescales from rotational diffusion constants was successfully fit to the overall rotational correlation functions from MD simulations for all individual N-H bonds. Furthermore, the new correlation functions calculated from Eq. 10 were in good agreement with the total correlation functions calculated from original trajectories. The results suggest that the intertia axes can be used to describe the overall rotational diffusion as a good approximation and that the assumption of separation of internal and overall rotational relaxation (Eq. **??**) is a good approximation for the studied proteins, as observed previously also for other protein [7, 21].

Using the new correlation functions from Eq. 10 in spin relaxation time calculations reduces the statistical fluctuations arising from longer lag times in correlation function calculation, which allows the higher accuracy with less simulation data. The essential reason is that the rotational diffusion constants can be determined by fitting a single parameter (linear slope) which is more robust than fitting exponential function with several parameters to a correlation function calculated from MD simulation. After determining the diffusion constants and using Eq. 10 the overall part of correlation functions do not have statistical fluctuations in spin relaxation time calculations.

Comparison to experimental results revealed that overall rotational diffusion coefficients were overestimated by a factor of ~ 3 in simulations with tip3p water, in agreement with previous studies [18, 19, 21]. Simulations with tip4p and opc4 water models gave more realistic diffusion coefficients, which overestimated diffusion only with factors ~ 1-1.2. The realistic overall rotational dynamics was determined by scaling the diffusion coefficients to all directions post-simulatively by the same constant factors such that the calculated T_1/T_2 was in optimal agreement with experiments. Similar correction has been done previously for proteins with isotropic rotational diffusion with single exponential rotational correlation function [7, 10–12, 48]. Alternatively only order parameters are used in the comparison with experiments [9, 12, 13, 48]. Overall rotational diffusion is previously corrected for anisotropic molecules by using isotropic reorientational eigenmode dynamics (iRED) [18] or quaternions [19]. The advantage of these approaches is that the separation between internal and overall rotational dynamics is not required, thus they would be applicable also for intrinsically disoredered proteins. However, the correction of overall rotational diffusion is based on the assumption that incorrect diffusion arises from incorrect water viscosity. Thus, a model with correct overall rotational diffusion is required to compare intrinsically disordered molecule simulations to experimental relaxation data.

A good agreement between spin relaxation times from experiments and simulations is found after overall rotational diffusion constants are scaled with a constant factor. This allows the interpretation of internal protein dynamics from spin relaxation times by using MD simulations even with tip3p water model. Here we use the approach to indentify dynamical regions in two proteins, HpTonB-92 and PsTonB with relatively rigid structures. However, the approach could be useful for intepretation of spin relaxation data from proteins with more regions containing complicated local dynamics, like Calmodulin [**?**].

[1] V. A. Jarymowycz and M. J. Stone, Chemical Reviews **106**, 1624 (2006).

[2] D. Korzhnev, M. Billeter, A. Arseniev, and V. Orekhov, Progress in Nuclear Magnetic Resonance Spectroscopy **38**, 197 (2001).

[3] V. den Bedem H and F. JS., Nat. Methods **12**, 307 (2015).

[4] J. R. Lewandowski, M. E. Halse, M. Blackledge, and L. Emsley, Science **348**, 578 (2015).

[5] J. M. Lamley, M. J. Lougher, H. J. Sass, M. Rogowski, S. Grzesiek, and J. R. Lewandowski, Phys. Chem. Chem. Phys. **17**, 21997 (2015).

[6] V. Kasinath, K. A. Sharp, and A. J. Wand, Journal of the American Chemical Society **135**, 15092 (2013).

[7] O. Allnr, N. Foloppe, and L. Nilsson, The Journal of Physical Chemistry B **119**, 1114 (2015).

[8] M. Akke, R. Brueschweiler, and A. G. Palmer, Journal of the American Chemical Society **115**, 9832 (1993).

[9] R. B. Best and M. Vendruscolo, Journal of the American Chemical Society **126**, 8090 (2004).

[10] S. A. Showalter and R. Brschweiler, Journal of Chemical Theory and Computation **3**, 961 (2007).

[11] S. A. Showalter, E. Johnson, M. Rance, and R. Brschweiler, Journal of the American Chemical Society **129**, 14146 (2007).

[12] P. Maragakis, K. Lindorff-Larsen, M. P. Eastwood, R. O. Dror, J. L. Klepeis, I. T. Arkin, M. . Jensen, H. Xu, N. Trbovic, R. A. Friesner, A. G. Palmer, and D. E. Shaw, The Journal of Physical

Chemistry B **112**, 6155 (2008).

[13] N. Trbovic, B. Kim, R. A. Friesner, and A. G. Palmer, Proteins: Structure, Function, and Bioinformatics **71**, 684 (2008).

[14] H. Wennerstroem, B. Lindman, O. Soederman, T. Drakenberg, and J. B. Rosenholm, Journal of the American Chemical Society **101**, 6860 (1979).

[15] G. Lipari and A. Szabo, J. Am. Chem. Soc. **104**, 4546 (1982).

[16] P. Luginbhl, K. V. Pervushin, H. Iwai, and K. Wthrich, Biochemistry **36**, 7305 (1997).

[17] J. Blake-Hall, O. Walker, and D. Fushman, "Characterization of the overall rotational diffusion of a protein from 15n relaxation measurements and hydrodynamic calculations," in *Protein NMR Techniques*, edited by A. K. Downing (Humana Press, Totowa, NJ, 2004) pp. 139–159.

[18] J. J. Prompers and R. Brschweiler, Journal of the American Chemical Society **124**, 4522 (2002).

[19] J. S. Anderson and D. M. LeMaster, Biophysical Chemistry **168**, 28 (2012).

[20] W. L. Jorgensen, J. Chandrasekhar, J. D. Madura, R. W. Impey, and M. L. Klein, J. Chem. Phys. **79**, 926 (1983).

[21] V. Wong and D. A. Case, The Journal of Physical Chemistry B **112**, 6013 (2008).

[22] C.-Y. Lu and D. A. V. Bout, The Journal of Chemical Physics **125**, 124701 (2006).

[23] P. Dosset, J.-C. Hus, M. Blackledge, and D. Marion, Journal of Biomolecular NMR **16**, 23 (2000).

[24] J. G. de la Torre, M. Huertas, and B. Carrasco, Journal of Magnetic Resonance **147**, 138 (2000).

[25] A. Abragam, *The Principles of Nuclear Magnetism* (Oxford University Press, 1961).

[26] L. E. Kay, D. A. Torchia, and A. Bax, Biochemistry **28**, 8972 (1989).

[27] D. E. Woessner, The Journal of Chemical Physics **37**, 647 (1962).

[28] $\tau_1 = (4D_{xx} + D_{yy} + D_{zz})^{-1}$, $\tau_2 = (D_{xx} + 4D_{yy} + D_{zz})^{-1}$, $\tau_3 = (D_{xx} + D_{yy} + 4D_{zz})^{-1}$, $\tau_4 = [6(D + (D^2 - L^2)^{-1/2}]^{-1}$, $\tau_5 = [6(D - (D^2 - L^2)^{-1/2}]^{-1}$, $D = \frac{1}{3}(D_{xx} + D_{yy} + D_{zz})$ and $L^2 = \frac{1}{3}(D_{xx}D_{yy} + D_{xx}D_{zz} + D_{yy}D_{zz})$.

[29] M. J. Abraham, T. Murtola, R. Schulz, S. Pll, J. C. Smith, B. Hess, and E. Lindahl, SoftwareX **12**, 19 (2015).

[30] K. Lindorff-Larsen, S. Piana, K. Palmo, P. Maragakis, J. L. Klepeis, R. O. Dror, and D. E. Shaw, Proteins: Structure, Function, and Bioinformatics **78**, 1950 (2010).

[31] S. Izadi, R. Anandakrishnan, and A. V. Onufriev, The Journal of Physical Chemistry Letters **5**, 3863 (2014).

[32] A. Ciragan, A. S. Aranko, I. Tascon, and H. Iwa, Journal of Molecular Biology **428**, 4573 (2016).

[33] G. Bussi, D. Donadio, and M. Parrinello, J. Chem. Phys. **126** (2007).

[34] M. Parrinello and A. Rahman, J. Appl. Phys. **52**, 7182 (1981).

[35] T. Darden, D. York, and L. Pedersen, J. Chem. Phys. **98**, 10089 (1993).

[36] U. L. Essman, M. L. Perera, M. L. Berkowitz, T. Larden, H. Lee, and L. G. Pedersen, J. Chem. Phys. **103**, 8577 (1995).

[37] B. Hess, J. Chem. Theory Comput. **4**, 116 (2008).

[38] M. Abraham, D. van der Spoel, E. Lindahl, B. Hess, and the GROMACS development team, *GROMACS user manual version 5.0.7* (2015).

[39] R. T. McGibbon, K. A. Beauchamp, M. P. Harrigan, C. Klein, J. M. Swails, C. X. Hernández, C. R. Schwantes, L.-P. Wang, T. J. Lane, and V. S. Pande, Biophysical Journal **109**, 1528 (2015).

[40] "Matlab, r2016a, the mathworks, inc., natick, massachusetts, united states.".

[41] A. Nowacka, N. Bongartz, O. Ollila, T. Nylander, and D. Topgaard, J. Magn. Res. **230**, 165 (2013).

[42] T. M. Ferreira, O. H. S. Ollila, R. Pigliapochi, A. P. Dabkowska, and D. Topgaard, J. Chem. Phys. **142**, 044905 (2015).

[43] V. Krishnan and M. Cosman, Journal of Biomolecular NMR **12**, 177 (1998).

[44] W. R. Carper and C. E. Keller, The Journal of Physical Chemistry A **101**, 3246 (1997).

[45] D. Frishman and P. Argos, Proteins: Structure, Function, and Bioinformatics **23**, 566 (1995).

[46] W. Humphrey, A. Dalke, and K. Schulten, Journal of Molecular Graphics **14**, 33 (1996).

[47] F. Hfling and T. Franosch, Reports on Progress in Physics **76**, 046602 (2013).

[48] Y. Gu, D.-W. Li, and R. Brschweiler, Journal of Chemical Theory and Computation **10**, 2599 (2014).
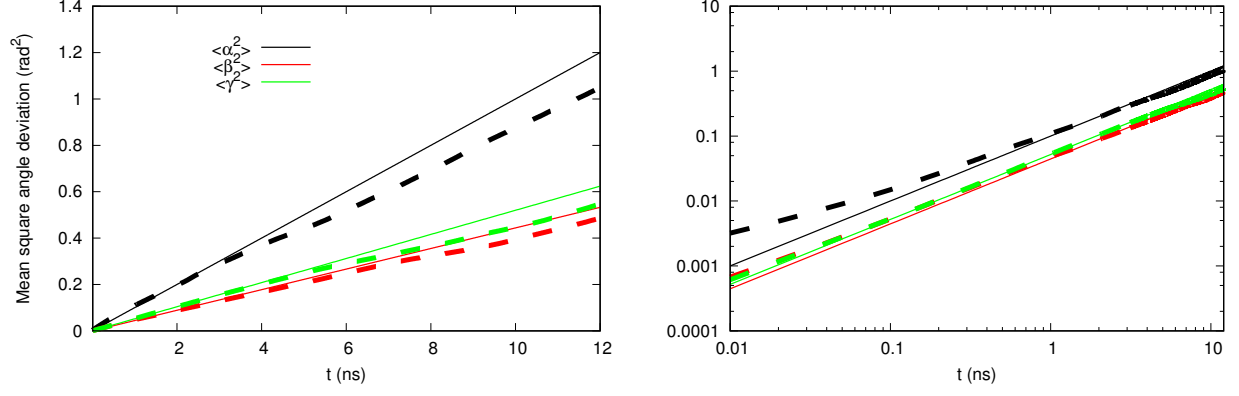
SUPPLEMENTARY INFORMATION

FIG. 8. The intertia tensor angles as a function of time and mean square angular deviations for PsTonB simulation with tip4p water model at 310K.
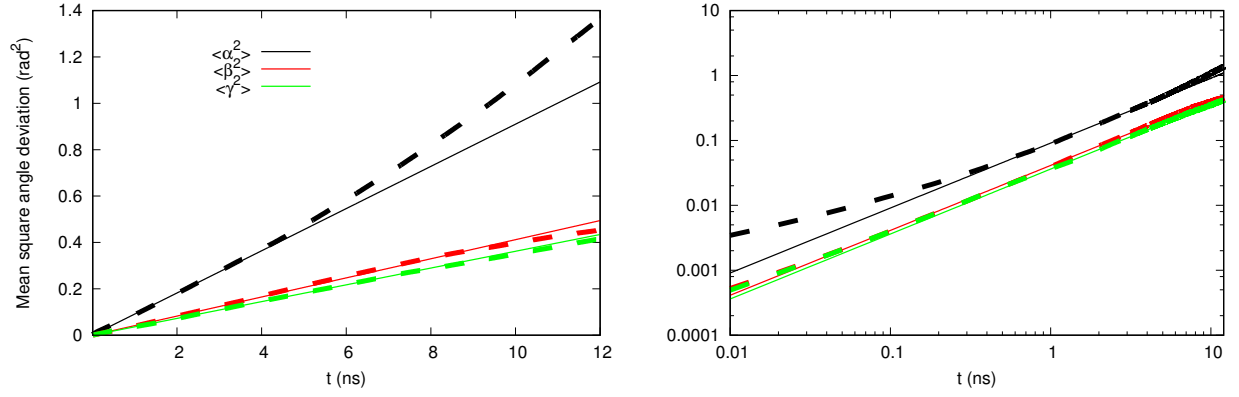

FIG. 9. The intertia tensor angles as a function of time and mean square angular deviations for PsTonB simulation with tip4p water model at 298K.